Diffusion in Ion Exchange Resins

BURTON HERING and HARDING BLISS

Yale University, New Haven, Connecticut

Observations on the rate of ion exchange in Dowex 50W resins are reported. These measurements were made under conditions where solid diffusion was the governing phenomenon for six pairs of ions sodium-zinc, sodium-silver, silver-aluminum, zinc-copper, zinc-aluminum, and aluminum-cerium (trivalent). The effects of temperature and of resin cross-linkage were studied with the first system. Exchange in both directions was studied for each pair except the last.

Interpretation with a Fick's law model was accomplished, and diffusion coefficients were obtained for each pair. Values were greatly dependent on the direction of the exchange as well as on the particular pair.

Interpretation with a Nernst-Planck model was also accomplished and diffusivities for each ion were obtained. Values were greatly influenced by the nature of the second ion except in the case of sodium. The interpretation in this case required numerical solution of the flux equations. These solutions are presented for valence ratios of 1/3 and 2/3 with diffusivity ratios of 5, 10, and 20 and for valence ratios of 3 and 3/2 with diffusivity ratios of 1/5, 1/10, and 1/20.

Activation energies were found to be 4 to 6 kcal/g. mole for either model. Increasing the resin cross-linkage from 4 to 12% decreased the diffusion values by approximately 80%.

The data were equally well represented with either model. In view of the simplicity of Fick's law, the use of this model is recommended for design purposes.

The kinetic behavior of ion exchange resins is of much theoretical and practical interest. The ultimate aim in the design of a fixed-bed ion exchange installation is the prediction of break-through curves for a particular set of conditions. Formerly, this was accomplished by the observation of breakthrough curves on a laboratory scale and the interpretation of these curves in terms of a suitable mathematical model to yield the fundamental parameters such as fluid-phase transfer coefficients and solid-phase diffusivity. This method has always suffered from the fact that the simplified assumptions, made so that the appropriate equations could be solved, were in varying degrees unrealistic. The advent of high-speed computers has made possible a reversal in this approach. One can now advantageously measure the pertinent parameters first and let the computer combine these with a minimum of assumptions into a predicted breakthrough curve.

One of the fundamental parameters is the diffusivity in the solid phase. The accurate measurement of this property becomes highly desirable, and such measurement was the aim of this work. The experimental method involves contacting resin beads with aqueous solutions for varying and known periods of time. The concentrations of solutions and amounts of resin are chosen in such a way that there is negligible concentration change in the solution during the exchange process. After the phases are separated, analysis of the resin permits determination of the appropriate diffusivity.

The resin studied was Dowex 50W. Exchange in both directions at 25°C. was measured for the following pairs of ions with a resin of 8% nominal cross-linkage (Dowex 50Wx8):

sodium (Na^+)	—	silver (Ag^+)
sodium (Na^+)	—	zinc (Zn^{++})
silver (Ag^+)	—	aluminum (Al^{+++})
zinc (Zn^{++})	—	copper (Cu^{++})
zinc (Zn^{++})	—	aluminum (Al^{+++})
aluminum (Al^{+++})	—	cerium (Ce^{+++})*

In addition, sodium-zinc exchange was studied with the Dowex 50Wx8 at 0° and 60°C. Sodium-zinc exchange was also measured at 25°C. with Dowex 50W of 4 and 12% nominal cross-linkage (Dowex 50Wx4 and Dowex 50Wx12).

EXPERIMENTAL

Size Separation

Since diameter of the resin particles is a quantity of great importance in governing the rate of exchange, it was necessary to make a fine cut in particle size. This was accomplished with an elutriation technique in which the resin particles were fluidized by a rising water column. The particles selected were those which flowed over the top of a 2.4-cm. I.D. column but did not flow over the top of a 2.6-cm. I.D. column in series with the first. Measurements of the wet, swollen resin diameters were made with a calibrated filar micrometer mounted on a microscope at 50X magnification. The standard deviations in the diameter of a 50-bead sample varied from 4.5 to 8.5% with most sets having deviations of less than 6%.

Ion Exchange Apparatus

The ion exchange apparatus is shown in Figure 1. The resin beads were held in a basket, *H*, 9.6-cm. I.D. × 19.2-cm. high, made of monofilament saran cloth. The weave was roughly equivalent to a 200-mesh screen. The basket was supported on a lucite frame, *A*, by means of the support rods, *J*. The frame provided strength and rigidity for the necessary auxiliaries. A baffle, *D*, made up of 5-mm. O.D. glass rods 15.2-cm. long which connected upper and lower ring plates, extended from the frame into the basket. A feed injector, *K*, made of 6-mm. I.D. glass tubing could be introduced through the slot, *B*. The stirrer, *G*, (motor, *E*) was introduced into the basket; its swirling motion was broken up by the baffles. A thermometer, L, projecting into the basket, was also carried on the lucite frame. Beakers, *M* of 3-liter capacity containing the exchanging solution could be brought up quickly around the basket and as quickly removed. Other beakers of 2-liter capacity were provided for wash water.

Procedure

Two to 3 grams of sized wet resin in a particular ionic form were charged to the feed injector. With the saran basket and thermometer in place, a beaker containing three liters of approximately one normal exchange solution was raised about the basket and the stirrer was started. The resin was injected, the time required being about 1 sec. After a predetermined contact time (measured with a stopwatch) had elapsed, the beaker was lowered and the solution drained from the basket while the resin was retained. Drainage time was about 2 sec. Another beaker with 2 liters of distilled water was quickly raised about the basket, and the beads were stirred in this water for 4 to 5 sec., thus stopping the exchange. This beaker

Burton Hering is with Esso Research and Engineering, Florham Park, New Jersey.

* In this case only the exchange of aluminum in solution for cerium on the resin was accomplished.

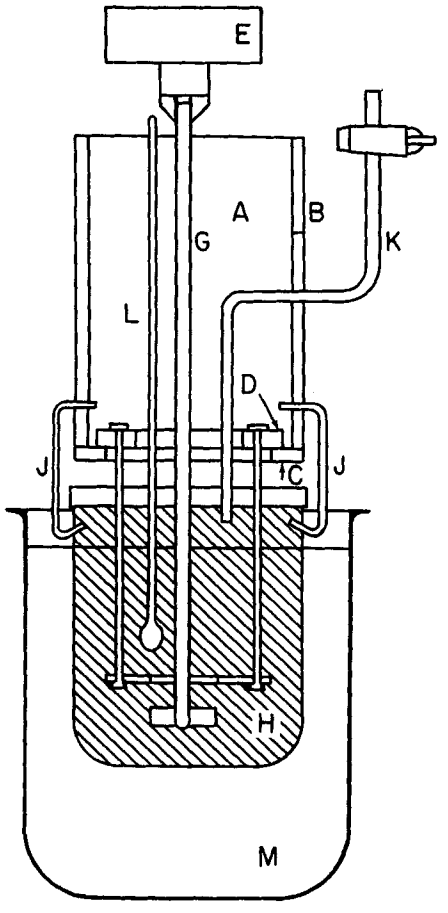

Fig. 1. Ion exchange equipment.

was lowered and replaced with a second 2-liter wash of 10-sec. duration. After the second wash the basket and beads were dropped into this beaker, the basket immediately removed, the water decanted, and the beads transferred and washed once more. The main exchange solution was used for seven or eight runs in succession without experiencing a more than 3% drop in concentration, a figure wholly negligible in its effect on the exchange rates.

The runs described above were short time runs for kinetic data. Equilibrium data were observed in the same way with runs of 2- to 12-hr. duration.

Most of the exchange runs were carried out at room temperature (25°C.). Runs at 60°C. were conducted with the beaker of exchange solution resting in a heating mantle, those at 0°C. with the beaker in an ice-salt bath. In all three cases, temperature control was to ± 1°C.

After the exchange process, the washed resin was swirled with about 10 ml. of water in a small beaker. This action resulted in broken or nonspherical beads adhering to the walls and this facilitated their removal. Repetition of this increased the sphericity of the sample from about 85 to greater than 95%. All analyses were made only on the latter material. The resin was dried by suction for 10 min. and by standing in air for 25 min. and then weighed. The resin was then contacted with 40 ml. of 10% sulfuric or nitric acid for 10 hr. at room temperature or 2 hr. at 60°C. The resin was filtered on a saran screen and then treated again with acid for ½ hr. After this treatment, a third acid replacement was accomplished in the same way and the resin finally washed. Occasionally, the resin was given a fourth replacement to test for completeness of the first three, but in all cases the three were shown to be sufficient. The replacement and wash solutions were combined for analysis.

Analyses

Zinc was determined by titration with potassium ferrocyanide in the presence of potassium ferricyanide using a diphenylamine indicator (*13*). Copper was determined by colorimetric methods (*17*) based on the tetramminecopper (II) ion complex with a colorimeter. Silver was analyzed by titration with potassium thiocyanate (*14*) using a ferric sulfate indicator. Trivalent cerium was determined by oxidizing it to tetravalent form with sulfuric acid, potassium peroxydisulfate, and silver nitrate and titrating the cerate solution with ferrous ammonium sulfate using diphenylamine as indicator (*16*). Sodium and aluminum were not analyzed directly; when these ions were the major ones on the resin, the minor ones were silver, zinc, or cerium. The minor ones could be analyzed and the sodium or aluminum calculated by difference from the known ultimate capacity.

Materials

Analytical or chemically pure reagents were used in all cases.

DATA

Exchange Runs

The detailed data on over 300 runs (each time point required one run) are given by Hering (*11*). A representative series is shown in Figure 2 in which the fractional approach to equilibrium is plotted vs. time. Since only the zinc and not the sodium on the resin was determined, the data appear as the amount of zinc picked up by the resin when zinc goes from solution to resin and as the amount of zinc retained in the resin when sodium goes from solution to resin. It should be noted that the fractional approach to equilibrium, $F = Q/Q^{\infty}$, vs. time is the basic observation on which all results of this work are based.

QUALITATIVE OBSERVATIONS ON THE DATA

Wet Resin Basis

All analyses of the resin phase yield the amount of ion on the solid per unit weight. The weight basis is, however, arbitrary. Recommended drying procedures (*5*) involving heating at 80°C. and subsequent rewetting of the resin resulted in excessive physical breakdown of the resin. A drying procedure involving the removal of surface moisture only by suction was evolved and shown to be entirely satisfactory in that wet resin weights were reproducible to 0.2%.* All compositions were thus ex-

* Variations in the internal water content with ionic composition of the resin can be appreciable. However, for the systems studied the error introduced into the observation of the fractional approach to equilibrium, $F = \frac{Q}{Q^{\infty}}$, is within the experimental accuracy of the data and, therefore, was neglected.

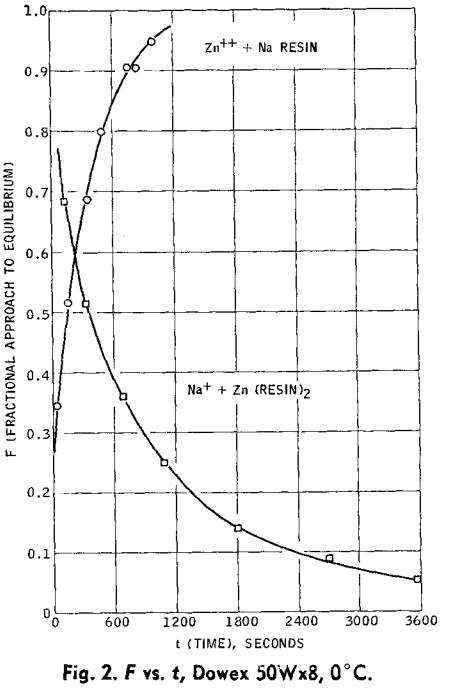

Fig. 2. F vs. t, Dowex 50Wx8, 0°C.

Table 1. Operating Equilibrium Capacities

System	Q^∞	No. of determinations	Standard deviation, %
Zn → Na	1.09 millimoles Zn/g. wet Na resin	25	3.7
Cu → Zn	1.22 millimoles Cu/g. wet Zn resin	5	3.9
Zn → Al	1.29 millimoles Zn/g. wet Al resin	6	1.6
Ag → Al	3.01 millimoles Ag/g. wet Al resin	4	1.7
Ag → Na	2.82 millimoles Ag/g. wet Na resin	2	2.8
Ce → Al	0.72 millimoles Ce/g. wet Al resin	5	2.8

pressed as milligrams of ion per gram of wet resin in a specified ionic form. This drying procedure did not result in resin deterioration, and the beads were repeatedly reused in subsequent experiments.

Operating Equilibrium Capacity

The equilibrium capacity of the resin for the exchanging ion in each ionic system was determined by measuring the amount exchanged in long-time (equilibrium) runs. These capacities, characterized by Q^∞, are shown in Table 1.

These values of Q^∞ may be converted to a common basis such as millimoles of zinc per gram of wet sodium resin. The results yield a Q^∞ in those units which varies from 1.05 to 1.25 in all systems except the two involving silver in which the values of 1.46 and 1.41 are calculated. These differences are unimportant, however, since the detailed interpretation of the data involved the fractional approach to equilibrium (Q/Q^∞), and this was always found in terms of the Q^∞ for the particular system at hand, that is, the values given in Table 1.

Reproducibility

Reproducibility of the data was explored systematically only for an initial test system, copper-hydrogen exchange. Runs were made with the hydrogen ion form of the resin and in copper solution. The exchange was about 85% complete in 65 sec. Repeated observations on the fractional approach to equilibrium at three different times showed that these observations were reproducible to within ± 5%. Since this figure is of the same order as the standard deviation in Q^∞, it appears that the major source of error is in the weighing and chemical analyses and not in time measurements, the only particular in which a determination of Q differs from that of Q^∞. Since the copper-hydrogen exchange was faster than all the others, the time errors here should have been the greatest of all the series.

Effect of Particle Diameter

The aim of this work was the measurement of solid-phase diffusivities. It was thus essential, at the outset, to establish that the observations showed behavior dependent on solid diffusivity and not on some other property or phenomenon. One way to do this was to measure the fractional approach to equilibrium vs. time for resins of different diameter. The results are shown in Figure 3. It is clear that the rate was reduced as the particle size was increased as should be the case with solid diffusion. Furthermore, since the time for a given fractional approach to equilibrium should be proportional to the square of the particle size [see Equation (1)], it should be possible to bring all these observations together into one line. This was done as is shown in Figure 4.

Resin samples with mean particle diameters of 0.069 to 0.094 cm. were used in this work. Within the limits of experimental accuracy, these particle diameters for the systems studied were not effected by temperature, the exchange solution used and its concentration, and the ionic form.

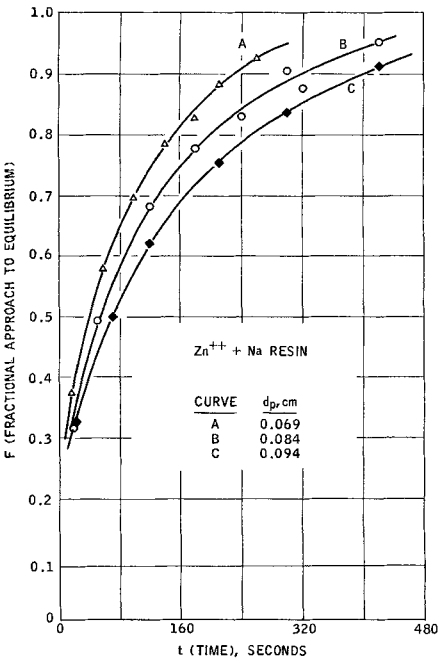

Fig. 3. Effect of particle diameter on F vs. t, Dowex 50Wx8, 25°C.

Effect of Stirrer Speed

The standard speed of stirring in this work was 440 rev./min. Higher speeds should not influence the behavior if solid diffusion were the rate-controlling mechanism, but they would be expected to influence it if fluid diffusion had some importance. The absence of effect at 930 rev./min. stirring is shown in Figure 4.

Effect of Cation Solution Concentration and the Nature of the Anion

It is obvious that the cation-solution concentration should be high in order to accelerate the fluid diffusion process and thus make more important the solid diffusion step. This was explored with zinc in nitrate solutions exchanging for sodium on Dowex 50Wx8. There seemed to be no effect in going from 0.2 to 1.0 normal zinc nitrate solutions as Figure 4 shows. Furthermore, results with 1.0 normal zinc sulfate (as distinct from nitrate) showed no effect.

In the reverse exchange, however, that is, sodium in chloride solutions exchanging for zinc on the resin, there was an effect in going from 0.2 to 1.0 normal. At 1.0 normal, however, the effect seemed to disappear, and this was confirmed with 1.0 normal sodium sulfate which yielded a line practically identical to 1.0 normal sodium chloride.

Thus 1.0 normal solutions were used throughout. It should be noted, however, that the effects of concentration and anion were measured only on the sodium-zinc system.

Interrupted Runs

Two sets of runs were carried out with batches of Dowex 50Wx8 in sodium form which had been initially contacted with 1.0 normal zinc sulfate solutions for 150 and 250 sec., respectively. After such contact the resins were separated from the solution, washed, and allowed to stand for a period of time. They were then brought again into contact with the zinc solutions. They began to exchange again at a considerably higher rate than that at which they had been exchanging at the interruption point. This is good evidence that a concentration gradient existed in the solid phase (an essential for solid diffusion control) and was equalized during the idle period. Similar conclusions were reached by Bieber, Steidler, and

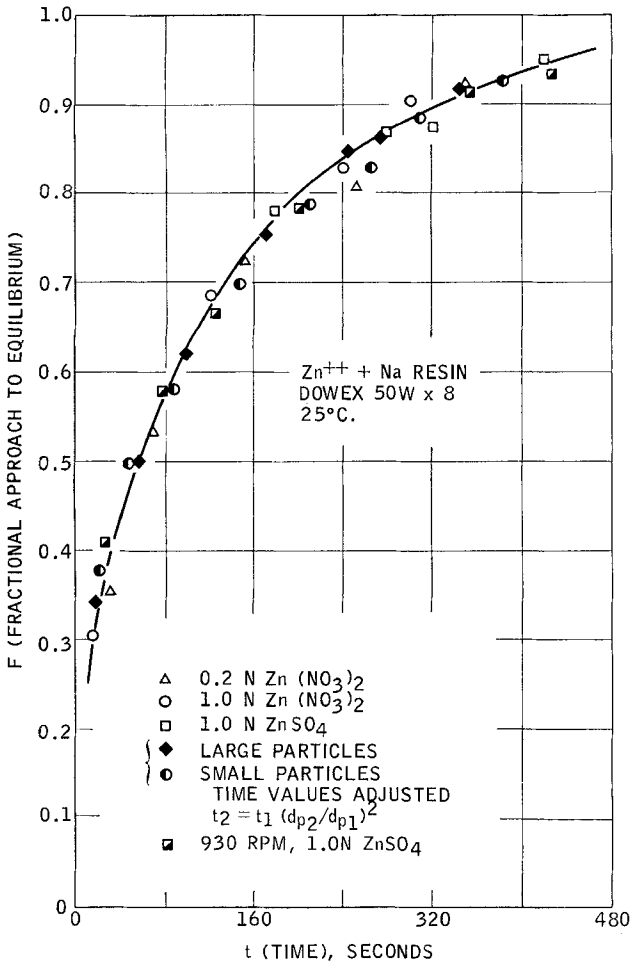

Fig. 4. Effect of solution concentration, solution anion, particle diameter and stirrer speed on F vs. t.

Selke (*1*) using shallow-bed studies. In this work, resistance in the fluid phase was also important.

Solid Diffusion as the Controlling Step

The various items above, that is, the effect of particle diameter, the negligible effect of stirrer speed above 440 rev./min., the negligible effect of solution cation concentration above 1.0 normal, the negligible effect of solution anion nature, and the behavior of the resin in interrupted runs, all point to the fact that solid diffusion is the controlling step in these observations. All these, except the last, are clearly shown in Figure 4. One can feel confident that the observations to be interpreted below are truly observations on solid diffusion, an assertion verified with the criterion of Helfferich (*8*).

THEORETICAL CONSIDERATIONS

Fick's Law Model

The conventional approach to diffusion is expressed by the well-known equation (*4*)

$$F = \frac{Q_B}{Q_{B^\infty}} = 1 - \frac{Q_A}{Q_{A^\infty}} = 1 - \frac{6}{\pi^2} \sum_{n-1}^{\infty} \frac{1}{n^2} \exp\left[-\frac{4D_{AB}\,\pi^2\,nt}{d_p^2}\right] \quad (1)$$

which is restricted to the case of constant solid surface concentration as is the case here. This condition is expressed by

$$(q_B)_{r=r_p} = q_{B^\infty} = Q_{B^\infty} \quad (2)$$

It should be noted that the diffusion coefficient, D_{AB}, represents the combined effects of A and B; it is not a characteristic of either A or B.

Nernst-Planck Model

The Fick's law model is an oversimplification of the phenomena involved in diffusion of electrolytes in solutions where the effect of an electrical potential created by the motion of the ions must be considered. Ions of high mobility diffuse quickly and establish an electrical charge gradient which tends to accelerate the slower ions and decelerate the faster ones. Since electroneutrality must be maintained, the fluxes of cations and anions are in the same direction and of the same magnitude on an equivalent basis.

Sulfonic acid cation exchange resins (Dowex 50W), in both the acid and salt forms, are highly ionized when placed in water. Anionic groups are fixed to the resin matrix and resist the entrance of solution anions into the resin. Within the ion exchange resin there is no electrical current flow so the net diffusion of counter cations must be zero. These phenomena are described in the Nernst-Planck equations (*9*)

$$-j_A = D_A\left[\nabla q_A + z_A q_A\left(\frac{F}{RT}\right)\nabla\psi\right] \quad (3)$$

$$-j_B = D_B\left[\nabla q_B + z_B q_B\left(\frac{F}{RT}\right)\nabla\psi\right] \quad (3a)$$

the absence of an electric current

$$z_A j_A + z_B j_B = 0 \quad (3b)$$

and the constant resin capacity

$$z_A q_A + z_B q_B = \text{a constant} \quad (3c)$$

Ion species A is that originally in the resin and B is that in solution. The constancy of D_A and D_B, the neglect of flux of anions and solvent, no interaction between cations other than electric forces, and the constancy of all activity coefficients are assumed in deriving these equations.

Equations (3) through (3c) may be combined and written as

$$-j_A = \frac{D_A D_B (z_A^2 q_A + z_B^2 q_B)}{D_A z_A^2 q_A + D_B z_B^2 q_B}\nabla q_A = D_{AB}\nabla q_A \quad (4)$$

analogous to the simple diffusion equation. When written in dimensionless terms for spherical symmetry, Equation (4) becomes

$$\frac{\partial G}{\partial \tau} = \frac{1}{\rho^2}\frac{\partial}{\partial \rho}\left[\frac{1+bG}{1+aG}\rho^2\frac{\partial G}{\partial \rho}\right] \quad (5)$$

The boundary conditions are

$$G = \frac{z_A q_A}{q_{A^\infty}} = 1 \text{ for } \tau = \left(\frac{4 D_A t}{d_p^2}\right) = 0 \quad (5a)$$

and

$$0 \leq \left(\rho = \frac{r}{r_p}\right) < 1$$

that is, the resin is initially entirely in A form except at the full radius, r_p, and $G = 0$ for $\rho = 1$ at all τ, that is, the resin is entirely saturated with B at the outer radius. This nonlinear differential equation can be solved numerically to yield $G(\tau,\rho)$, and the fractional approach to equilibrium is then evaluated with the equation

$$F = \frac{Q_B}{Q_{B^\infty}} = 1 - \frac{Q_A}{Q_{A^\infty}} = 1 - 3\int_0^1 G(\tau,\rho)\rho^2\,d\rho \quad (6)$$

Helfferich, Plesset, and Franklin (*9, 10*) have presented the solution to Equations (5) and (6) for the following cases:

TABLE 2. F (FRACTIONAL APPROACH TO EQUILIBRIUM) VS. $\tau = \left(\frac{4 D_A t}{d_p^2}\right)$

Nernst-Planck Model

	$\frac{z_A}{z_B} = \frac{1}{3}$			$\frac{z_A}{z_B} = 3$		
	$\frac{D_A}{D_B} = 5$	$\frac{D_A}{D_B} = 10$	$\frac{D_A}{D_B} = 20$	$\frac{D_A}{D_B} = \frac{1}{5}$	$\frac{D_A}{D_B} = \frac{1}{10}$	$\frac{D_A}{D_B} = \frac{1}{20}$
F	τ	τ	τ	τ	τ	τ
0.05	0.000355	0.000458	0.000648	0.000108	0.000088	0.000073
0.10	0.00142	0.00196	0.00302	0.000438	0.000356	0.000310
0.15	0.00339	0.00475	0.00702	0.00103	0.000844	0.000723
0.20	0.00617	0.00833	0.0121	0.00191	0.00156	0.00134
0.30	0.0147	0.0198	0.0283	0.00463	0.00378	0.00327
0.40	0.0280	0.0372	0.0528	0.00901	0.00741	0.00644
0.50	0.0470	0.0625	0.0878	0.0156	0.0129	0.0114
0.60	0.0740	0.0978	0.1368	0.0254	0.0213	0.0190
0.70	0.1118	0.1468	0.2048	0.0402	0.0345	0.0314
0.80	0.1673	0.2178	0.3018	0.0650	0.0573	0.0531
0.85	0.2053	0.2668	0.3668	0.0850	0.0760	0.0712
0.90	0.2573	0.3308	0.4528	0.1158	0.1055	0.1001
0.95	0.3393	0.4268	0.5768	0.1744	0.1628	0.1567
0.99	0.5143	0.6128	0.7868	0.3302	0.3173	0.3105

Ion valence ratio $\frac{z_A}{z_B} = 1; \frac{D_A}{D_B} = 2, 5, 10, 1/2, 1/5, 1/10$

Ion valence ratio $\frac{z_A}{z_B} = 1/2; \frac{D_A}{D_B} = 5, 10, 20$

Ion valence ratio $\frac{z_A}{z_B} = 2; \frac{D_A}{D_B} = 1/5, 1/10, 1/20$

The additional valence cases 3 to 1 and 3 to 2 were of interest in this work. Accordingly, Equation (5) was written in finite difference form and solved and the integral in (6) evaluated with Simpson's rule.* This work was done by Hering (*11*) and is reported fully by him. Solution was accomplished for the following cases:

* Calculations were carried out using the IBM-709 digital computer at Massachusetts Institute of Technology, Cambridge, Massachusetts.

Ion valence ratio $\frac{z_A}{z_B} = 1/3, 2/3; \frac{D_A}{D_B} = 5, 10, 20$

Ion valence ratio $\frac{z_A}{z_B} = 3, 3/2; \frac{D_A}{D_B} = 1/5, 1/10, 1/20$

The results are presented in Tables 2 and 3. These tables are condensed; more entries are given by Hering (*11*).

It should be noted that the ratio $\frac{D_A}{D_B} = 1.0$ for any valence ratio can be shown to be equivalent to Fick's law.

INTERPRETATION OF DATA

Weighting of Data Points

There is no doubt that errors in time measurements are greatest in those runs at very short times (lowest

TABLE 3. F (FRACTIONAL APPROACH TO EQUILIBRIUM) VS. $\tau = \left(\frac{4 D_A t}{d_p^2}\right)$

Nernst-Planck Model

	$\frac{z_A}{z_B} = \frac{2}{3}$			$\frac{z_A}{z_B} = \frac{3}{2}$		
	$\frac{D_A}{D_B} = 5$	$\frac{D_A}{D_B} = 10$	$\frac{D_A}{D_B} = 20$	$\frac{D_A}{D_B} = \frac{1}{5}$	$\frac{D_A}{D_B} = \frac{1}{10}$	$\frac{D_A}{D_B} = \frac{1}{20}$
F	τ	τ	τ	τ	τ	τ
0.05	0.000419	0.000605	0.000965	0.000129	0.000113	0.000103
0.10	0.00176	0.00272	0.00463	0.000546	0.000475	0.000431
0.15	0.00409	0.00617	0.00996	0.00126	0.00110	0.00100
0.20	0.00740	0.0109	0.0172	0.00232	0.00202	0.00184
0.30	0.0174	0.0253	0.0390	0.00560	0.00489	0.00446
0.40	0.0330	0.0474	0.0720	0.0108	0.00952	0.00871
0.50	0.0554	0.0789	0.1190	0.0187	0.0166	0.0153
0.60	0.0869	0.1232	0.1842	0.0303	0.0271	0.0253
0.70	0.1309	0.1847	0.2752	0.0479	0.0435	0.0411
0.80	0.1949	0.2732	0.4042	0.0767	0.0709	0.0678
0.85	0.2389	0.3332	0.4912	0.0993	0.0928	0.0893
0.90	0.2979	0.4112	0.6032	0.1338	0.1263	0.1224
0.95	0.3889	0.5262	0.7622	0.1970	0.1887	0.1844
0.99	0.5709	0.7312	1.012	0.3580	0.3489	0.3442

values of F, fractional approach to equilibrium). Since the relative error in F is approximately constant, the absolute error is greatest at large values of F. Thus, those data points involving F between 0.7 and 0.93 were weighted more heavily than values outside this range in the interpretation to follow.

Nernst-Planck Model

The experimental data were first plotted as F, fractional approach to equilibrium of the ion originally in solution, B, vs. time. These data were then smoothed with a 5-point least squares approximation for a cubic equation of the form

$$\ln (1 - F^2) = a't + b't^2 + c't^3 + d' \qquad (7)$$

Helfferich (9) suggested a similar expression for approximating ion exchange data. A comparison between smoothed F vs. t and theoretical F vs. τ curves was then required. Simple superposition proved unsuccessful because the curves for any one valence ratio were quite similar in slope within the experimental range of F for all the various diffusivity ratios. Equally unsuccessful were methods involving comparing F vs. $\frac{t}{t_o}$ or $\frac{F}{F_o}$ vs. $\frac{t}{t_o}$ in which F_o and t_o were arbitrarily chosen coordinates with the corresponding τ/τ_o values from the various theoretical curves. No unequivocal values of D_A and D_B could be found by these methods.

A cross-plot technique was finally evolved, a method which requires that data for exchange in both directions be available and which is based on the assumption that D_A and D_B are independent of the direction of the exchange. F values between 0.5 and 0.95 were tabulated for the exchange in one direction with the appropriate experimental time values from the smoothed data. For these values of F, the corresponding values of τ were read from the appropriate (that is, proper valence ratio) theoretical curves for each of the three known diffusivity ratios as well as for the equal diffusivities case (equivalent to Fick's law model). Since

$$D_A = \frac{d_p^2 \tau}{4t} \qquad (8)$$

D_A could be computed at each value of F for the four diffusivity ratios and an average (for all the values of F) of D_A was determined for each of these ratios. The variation in D_A with F was random. A plot of D_A vs. $\alpha = \frac{D_A}{D_B}$ was then made.

The same procedure was then applied to smoothed data for the reverse exchange and values of D_A' calculated for each of the four diffusivity ratios. A plot of D_A' vs. $\frac{1}{\alpha}$ was then made on the previous plot. The intersection of the two lines gave the best value of D_A, α, and thus D_B. It should be noted that this method yields a result in which $\alpha = \frac{D_A}{D_B}$ may have values other than the simple, integral ones for which the original theoretical F vs. τ curves were derived. This requires that interpolation curves of F vs. α at constant τ be constructed.

The final operation is one of comparing the original data with results computed from the Nernst-Planck model with the values of D_A and D_B found. Such a comparison is shown in Figure 5 for sodium-zinc exchange in both directions.

Fick's Law Model

Interpretation of the data according to this model was simple. Experimental values of F and t were substituted into Equation (1) and D_{AB} was calculated. Reichenberg (15) has described this procedure in detail. Average diffusion coefficients, D_{AB}, were determined for the exchanges in each direction, and comparison of the results of this case with measured data are also shown in Figure 5. Mathematically, the values of D_{AB} are equal to D_A of the Nernst-Planck model for $\alpha = 1$.

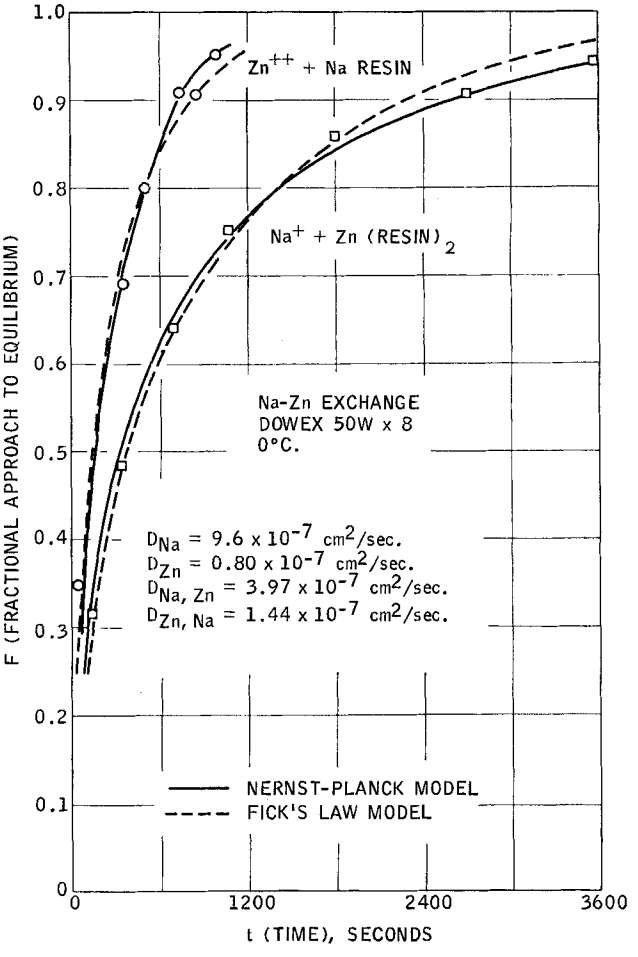

Fig. 5. Application of the Nernst-Planck and Fick's law models.

RESULTS AND DISCUSSION

The values of D_A and D_B (Nernst-Planck model) and D_{AB} and D_{BA} (Fick's law model) are given in Table 4.

Estimation of Errors

Since the Fick's law model can be expressed in a compact equation, it is possible to estimate the propagation of error with the usual methods applied to the first term in the series. The standard deviation for particle diameter was 6% for all resins except Dowex 50Wx12 where the figure was 9%. The standard deviation of F was from 1 to 19% depending on the particular series under consideration. The deviations in time were neglected, since time errors should be small in the F range of 0.7 to 0.93 as previously noted. The propagation of these errors in d_p and F was calculated for each series; the errors thus computed varied from 15 to 20%. These are tabulated in Table 4. They are assumed to be the same for the Nernst-Planck model.

Agreement Between Data and Theory

The standard deviations between experimental data and theoretical curves were determined for both models with the equation

TABLE 4. TABULATED RESULTS

Conditions	System ions	Ion valences	Dowex 50W resin cross-linkage % DVB	Temperature °C.	Nernst-Planck model $D \times 10^7$ sq. cm./sec.	α*	σ‡ Data from theory ±	Fick's law model† $D \times 10^7$ sq. cm./sec.	σ‡ Data from theory ±
A	Na	1	8	25	$D_{Na} = 20.3$	8.8	0.021	$D_{Na,Zn} = 9.71$	0.021
	Zn	2			$D_{Zn} = 2.31$ ±20%		0.012	$D_{Zn,Na} = 3.95$ ±20%	0.016
B	Na	1	8	0	$D_{Na} = 9.6$	12	0.029	$D_{Na,Zn} = 3.97$	0.025
	Zn	2			$D_{Zn} = 0.80$ ±20%		0.015	$D_{Zn,Na} = 1.44$ ±20%	0.015
C	Na	1	8	60	$D_{Na} = 38.3$	5.6	0.064	$D_{Na,Zn} = 22.2$	0.063
	Zn	2			$D_{Zn} = 6.84$ ±20%		0.013	$D_{Zn,Na} = 10.6$ ±20%	0.015
D	Na	1	4	25	$D_{Na} = 52.5$	13.2	0.038	$D_{Na,Zn} = 21.0$	0.035
	Zn	2			$D_{Zn} = 3.98$ ±15%		0.015	$D_{Zn,Na} = 7.15$ ±15%	0.019
E	Na	1	12	25	$D_{Na} = 7.34$	8	0.036	$D_{Na,Zn} = 3.74$	0.030
	Zn	2			$D_{Zn} = 0.92$ ±20%		0.021	$D_{Zn,Na} = 1.60$ ±20%	0.032
F	Na	1	8	25	$D_{Na} = 20.5$	3	0.058	$D_{Na,Ag} = 14.3$	0.051
	Ag	1			$D_{Ag} = 6.83$ ±20%		0.051	$D_{Ag,Na} = 8.6$ ±20%	0.061
G	Ag	1	8	25	$D_{Ag} = 3.80$	3.4	0.063	$D_{Ag,Al} = 2.98$	0.059
	Al	3			$D_{Al} = 1.12$ ±15%		0.025	$D_{Al,Ag} = 1.80$ ±15%	0.032
H	Cu	2	8	25	$D_{Cu} = 2.81$	1.8	0.016	$D_{Cu,Zn} = 2.30$	0.022
	Zn	2			$D_{Zn} = 1.57$ ±20%		0.011	$D_{Zn,Cu} = 1.81$ ±20%	0.012
I	Zn	2	8	25	$D_{Zn} = 0.710$	1.1	0.020	$D_{Zn,Al} = 0.692$	0.022
	Al	3			$D_{Al} = 0.645$ ±15%		0.017	$D_{Al,Zn} = 0.648$ ±15%	0.020
J	Al	3	8	25	$D_{Al} = 0.455$	—	—	—	—
	Ce**	3			$D_{Ce} = 0.091$ ±17%		0.035	$D_{Ce,Al} = 0.120$ ±17%	0.025

* $\alpha = \frac{D_{Na}}{D_{Zn}}, \frac{D_{Na}}{D_{Ag}}, \frac{D_{Ag}}{D_{Al}}, \frac{D_{Zn}}{D_{Cu}}, \frac{D_{Zn}}{D_{Al}}, \frac{D_{Al}}{D_{Ce}}$.

† The first subscript refers to the ion on the resin initially.

‡ σ is the standard deviation of the experimental data from the theoretical curve expressed in the scale of F.

** Only data for the exchange of Ce^{+3} on the resin initially were available. The values of D_{Al} and D_{Ce} were obtained by assuming $D_{Al}/D_{Ce} = 5$.

$$\sigma^2 = \frac{\sum_n (F_n - F_n^*)^2}{n - 1} \qquad (9)$$

which assumes no error in contact time. These figures are also given in Table 4. No distinction between the two models on this score is possible, that is, both models fit the data equally well.

Nernst-Planck Model

It is clear, from a study of Table 4 that the diffusivity of each ion is quite different from that of any other ion. It is also clear that the diffusivity of sodium when exchanging with zinc (conditions A) is about the same as its value when exchanging with silver (conditions F). This observation, however, is not true for any other ion. The diffusivity of silver when exchanging with sodium is different from that when exchanging with aluminum (conditions F and G). The diffusivity of zinc when exchanging with sodium is different from that when exchanging with copper and from that when exchanging with aluminum (conditions A, H, and I). The diffusivity of aluminum when exchanging with zinc is different from that when exchanging with cerium (conditions I and J) although the assumption that $\alpha = 5$ in the cerium case introduces uncertainty. Thus, it must be concluded that the diffusivities of the ions are, in general, influenced by the nature of the other ion.

Helfferich (7) found that a value of $D_{Na} = 35 \times 10^{-7}$ sq. cm./sec. determined from conductivity measurements could be used with an appropriate value for hydrogen to predict the behavior he observed in ion exchange. The resin he used was so greatly different from that used here that no more detailed comparison is possible. It should be noted that Helfferich's data can be interpreted equally well with the Fick's law model.

Comparison with other data in the literature is difficult, because most literature data were interpreted with the Fick's law model only. Comparison with self-diffusion coefficients should be valid, however. $D_{Na,Na}$ determined by Boyd and Soldano (2) in self-diffusion experiments with a sulfonic acid resin of about 8% cross-linkage at 25°C. was about 9×10^{-7} sq. cm./sec., while the D_{Na}

values reported here were about 20×10^{-7} when exchanging with zinc or silver. $D_{Zn,Zn}$ determined in self-diffusion experiments (2) at similar cross-linkage and temperature was 0.63×10^{-7}, while D_{Zn} reported here varies from 0.71 to 2.3×10^{-7} depending on the other ion. $D_{Ag,Ag}$ determined in self-diffusion experiments (2) at comparable conditions was 6.4×10^{-7} sq. cm./sec., while D_{Ag} reported here varied from 3.8 to 6.8×10^{-7} depending on the other ion. Boyd and Soldano (3) noticed a decrease in $D_{Na,Na}$ and an increase in $D_{Zn,Zn}$ when self-diffusion was studied with a solution in equilibrium with resin of 67.3% sodium and 32.7% zinc. They suggested a possible steric effect which could also explain the results of the present study.

The effect of resin cross-linkage is clearly shown for the sodium-zinc system (conditions *D, A, E*). The diffusivities of both ions are greatly decreased by increased resin cross-linkage as also found by Boyd and Soldano (2). A semilog plot of D vs. cross-linkage was made and D_{Na} was extrapolated to zero cross-linkage. The result is almost the same as that for sodium diffusion in concentrated aqueous solutions, $D^o_{Na} = 1.48 \times 10^{-5}$ sq. cm./sec. (12). The same extrapolation made for D_{Zn} yields a value of D^o_{Zn} only about one-tenth that reported for concentrated aqueous solutions (6).

The effect of temperature is shown in Table 4 for the sodium-zinc system (conditions *B, A, C*). The diffusivities of both ions are clearly increased at higher temperatures. The activation energies were 4 to 6 kcal./g. mole, entirely comparable to the results of Boyd and Soldano (2) in self-diffusion experiments.

Fick's Law Model

The diffusion coefficients D_{AB} or D_{BA} determined according to the Fick's law model are shown also in Table 4. The most notable observation is that these depend markedly, for the same system, on the direction of the exchange. The coefficient is lower when the ion initially on the resin was that with lower diffusivity as determined with the Nernst-Planck model. This is evident in all systems except zinc-aluminum where the diffusion coefficients in both directions are about the same. It is also clear, as would be expected, that the diffusion coefficient of a pair of ions is very much dependent on the particular pair, for example, $D_{Na,Zn}$ is quite different from $D_{Na,Ag}$. Comparison with literature values is difficult because so little pertinent data are available. No comparison with self-diffusion coefficients is meaningful in this case.

The effects of resin cross-linkage and of temperature found with this model were essentially the same as those found with the Nernst-Planck model.

Comparison of the two models

There is no doubt that the Nernst-Planck model is superior in theory to the Fick's law model. Indeed, the Nernst-Planck model was used to predict the dependence of the overall diffusion coefficient on the direction of exchange (7), that is, D_{AB} is larger when the faster ion is on the resin initially. The Fick's law model is unable to explain this effect. The Nernst-Planck model, however, does not fit the data any better. Furthermore, since the diffusivity of one ion is in general dependent on the other ion present, the model is capable of no more generality of result than the Fick's law model. Under these circumstances and because of the greater ease of using it in fixed-bed design calculations, a slight preference for the Fick's law model must be expressed.

CONCLUSIONS

The experimental equipment and procedure described proved to be an accurate means of determining diffusivities in ion exchange resins. Six pairs of ions constituting all combinations of +1, +2, and +3 ionic valences were studied with Dowex 50W. Data were interpreted by means of the Nernst-Planck and Fick's law models.

The effects of temperature and resin cross-linkage on ion exchange rates were comparable to those found by other investigators. Diffusivities of individual cations determined by the Nernst-Planck model also showed that in most cases there was a dependency on the nature of the second cation. A Fick's law interpretation led to diffusion coefficients influenced by the characteristics of the ions and the direction of exchange.

Both the Nernst-Planck and Fick's law models represented the results of this study adequately and equally well. The Nernst-Planck model provides a more meaningful description of the diffusion phenomenon while the Fick's law model is more suitable to methods presently available for the design of commercial ion exchange columns.

ACKNOWLEDGMENT

Burton Hering gratefully acknowledges the financial assistance of the E. I. du Pont de Nemours Company. The calculations presented were carried out in part at the Computation Center, Massachusetts Institute of Technology, Cambridge, Massachusetts.

NOTATION

A = cation initially on the resin
a = $(z_A D_A / z_B D_B) - 1$
a', b', c', d' = constants of Equation (7)
B = cation initially in solution
b = $(z_A / z_B) - 1$
D_A, D_B = ion diffusivities on resin, sq. cm./sec.
D^o_A, D^o_B = ion diffusivities in aqueous solution, sq. cm./sec.
$D_{A'}$ = diffusivity of A calculated from reverse exchange data, sq. cm./sec.
D_{AB}, D_{BA} = diffusion coefficients, sq. cm./sec.; first letter of subscript indicates ion initially on resin
d_p = particle diameter, cm.
F = fractional approach to equilibrium
F^* = theoretical fractional approach to equilibrium
G = $z_A q_A / q_A^\infty$
j_A, j_B = mole flux per unit area, millimoles/sec./sq. cm.
n = integer used in summation terms
Q_A, Q_B = total ion concentration in resin, millimoles/g. wet resin
Q_A^∞, Q_B^∞ = total ion concentration at equilibrium, millimoles/g. wet resin
q_A, q_B = point ion concentration in resin, millimoles/g. wet resin
q_A^∞, q_B^∞ = point ion concentration at equilibrium, millimoles/g. wet resin
R = gas constant
r = radial position in a resin sphere
r_p = particle radius, cm.
T = absolute temperature, °K.
t = contact time, sec.
z_A, z_B = ion valence
F = Faraday's constant

Greek Letters

∇ = gradient operator
α = D_A / D_B
ρ = r / r_p
σ = standard deviation
τ = $4 D_A t / d_p^2$
ψ = electrical potential

LITERATURE CITED

1. Bieber, Herman, F. E. Steidler, and W. A. Selke, *Chem. Eng. Progr. Symposium Ser. No. 14*, **50**, p. 17-21 (1954).
2. Boyd, G. E., and B. A. Soldano, *J. Am. Chem. Soc.*, **75**, 6091-6099 (1953).
3. *Ibid.*, pp. 6107-6110 (1953).
4. Crank, J., "The Mathematics of Diffusion," Oxford University Press, London (1957).
5. "Dowex: Ion Exchange," the Dow Chemical Company, Midland, Michigan (1958).
6. Hamer, W. J., ed., "The Structure of Electrolytic Solutions," Wiley, New York (1959).
7. Helfferich, Friedrich, *J. Phys. Chem.*, **66**, 39-43 (1962).
8. ———, "Ion Exchange," p. 255, McGraw-Hill, New York (1962).
9. Helfferich, Friedrich, and M. S. Plesset, *J. Chem. Phys.*, **28**, 418-424 (1958).
10. ———, and J. N. Franklin, *ibid.*, **29**, 1064-1069 (1958).
11. Hering, Burton, D. Eng. dissertation, Yale University, New Haven, Connecticut (1961).
12. "International Critical Tables," Vol. 5, pp. 65-67, McGraw-Hill, New York (1929).
13. Kolthoff, I. M., and E. B. Sandell, "Textbook of Qualitative Inorganic Analysis," pp. 549-551, Macmillan, New York (1952).
14. Pierce, W. C., and E. L. Haenisch, "Qualitative Analysis." Wiley, New York (1953).
15. Reichenberg, D., *J. Am. Chem. Soc.*, **75**, 589-597 (1953).
16. Smith, G. F., "Cerate Oxidimetry," The G. Frederick Smith Chemical Co., Columbus, Ohio (1942).
17. Snell, F. D., and C. T. Snell, "Colorimetric Methods of Analysis," Chap. 5, 17, Van Nostrand, New York (1949).

Manuscript received October 12, 1962; revision received January 23, 1963; paper accepted January 23, 1963.

An Analysis of Slug Flow Heat Transfer in an Eccentric Annulus

WILLIAM T. SNYDER

Brookhaven National Laboratory, Upton, New York

A solution is presented for the temperature distribution in a fluid flowing in an eccentric annulus formed with circular cylinders under the assumption of slug flow. The flow is assumed to be fully developed thermally with constant thermophysical properties. The outer surface is assumed to be adiabatic and the inner surface temperature is assumed to be independent of circumferential position. General expressions and numerical results for a typical set of conditions are presented for the quantities, local heat flux, local heat transfer coefficient, adiabatic surface temperature distribution, and average Nusselt number. The application of the present results to the prediction of turbulent heat transfer to liquid metals is indicated, and a comparison with other liquid metal heat transfer analyses is presented.

One of the critical problems encountered in the longitudinal flow in close-packed tubular heat exchangers is that of tube misalignment. For example, Friedland, Dwyer, Maresca, and Bonilla (*1*) observed variations by a factor of 2 to 4 of the average Nusselt number between different tubes in such an array. These investigators attributed this variation principally to the effect of tube misalignment in an initially geometrically symmetrical array.

An exact solution for the laminar flow velocity and temperature distributions between cylinders arranged in symmetrical triangular or square arrays has been presented by Sparrow and Loeffler (*2*, *3*). Deissler and Taylor (*4*) have analyzed the turbulent flow case using an approximate graphical technique. Dwyer and Tu (*5*) have presented an approximate analysis for turbulent flow heat transfer through bundles in which the model of an annulus was assumed. In this model, the hexagonal section associated with each tube is replaced by an imaginary annulus surrounding the tube such that the cross-sectional area of the annulus equals the hexagonal cross-sectional area associated with each tube. Sparrow and Loeffler (*3*) showed that for laminar flow, the approximate annulus model predicts the average Nusselt number with an error of less than 5% from the exact value for tube-spacing ratios (ratio of tube center distance to tube diameter) as low as 1.5. The error becomes even less at higher spacing ratios, and for turbulent flow, the error would be less than that for laminar flow at the same spacing ratio.

This background for the symmetric case suggests the use of an eccentric annulus as a model representative of the flow around a misaligned tube in an otherwise symmetric array. The purpose of the present investigation is to analyze the temperature distribution in an eccentric annulus assuming slug flow. Hartnett and Irvine (*6*) have shown that the slug flow Nusselt number is useful in estimating the total Nusselt number for liquid metals flowing in noncircular passages.

In the analysis, a thermally fully developed flow will be assumed with constant heat rate per unit length of the inner surface. The outer surface will be assumed to be adiabatic. The temperature on the inner surface will be assumed to be independent of circumferential position. As pointed out by Hartnett and Irvine (*6*), these boundary conditions represent one of three classes of boundary conditions of technical interest in noncircular duct heat transfer.

William T. Snyder is with the State University of New York, Stony Brook, New York.